New constraints on the origin of the Sierra Madre de Chiapas (south Mexico) from sediment provenance and apatite thermochronometry

C. Witt, S. Brichau, A. Carter

New constraints on the origin of the Sierra Madre de Chiapas (south Mexico) from sediment provenance and apatite thermochronometry

C. Witt,[1] S. Brichau,[2,3] and A. Carter[2]

Received 24 April 2012; revised 18 September 2012; accepted 26 September 2012; published 3 November 2012.

[1] The timing and source of deformation responsible for formation of the Sierra Madre de Chiapas (south Mexico) are unclear. To address this, apatite fission track and U-Th-He thermochronometry, combined with zircon U-Pb dating, were performed on bedrock and sedimentary samples of the Sierra Madre de Chiapas to discern timing of exhumation and identify sediment source areas. The U-Pb results show that Paleocene–Eocene terrigenous units outcropping at the northern section of the Sierra were mostly derived from Grenville (~1 Ga) basement whereas the internal sections of the chain yield mainly Permian to Triassic ages (circa 270–230 Ma) typical of the Chiapas massif complex. Grenville-sourced sediments are most probably sourced by the Oaxacan block or the Guichicovi complex and were deposited to the north of the Sierra in a foreland setting related to a Laramide deformation front. Other possibly source areas may be related to metasedimentary units widely documented at the south Maya block such as the Baldi unit. The apatite fission track and U-Th-He data combined with previously published results record three main stages in exhumation history: (1) slow exhumation between 35 and 25 Ma affecting mainly the Chiapas massif complex; (2) fast exhumation between 16 and 9 Ma related to the onset of major strike-slip deformation affecting both the Chiapas massif complex and Chiapas fold-and-thrust belt; and (3) a 6 to 5 Ma period of rapid cooling that affected the Chiapas fold-and-thrust belt, coincident with the landward migration of the Caribbean–North America plate boundaries. These data suggest that most of the topographic growth of the Sierra Madre de Chiapas took place in the middle to late Miocene. The new thermochronological evidence combined with stratigraphic and kinematic information suggests that the left-lateral strike-slip faults bounding the Chiapas fold-and-thrust belt to the west may have accommodated most of the displacement between the North American and Caribbean plates during the last 6–5 Ma.

Citation: Witt, C., S. Brichau, and A. Carter (2012), New constraints on the origin of the Sierra Madre de Chiapas (south Mexico) from sediment provenance and apatite thermochronometry, *Tectonics*, *31*, TC6001, doi:10.1029/2012TC003141.

1. Introduction

[2] Formation of the Sierra Madre de Chiapas (SMC), located in southern Mexico, close to the triple junction between the Cocos, Caribbean and North American plates (Figure 1) is not well understood. Two models emphasize the importance of strike-slip tectonics [*Guzmán-Speziale and Meneses-Rocha*, 2000; *Andreani et al.*, 2008a, 2008b] and suggest that exhumation along the SMC may have resulted from the transpressive component of deformation resulting from the change in trend of the major crustal faults that accommodate the relative motion between the North American and Caribbean plates (i.e., from the E-W directed Polochic-Motagua fault system, PMFS, to the NW-SE faults at the SMC; Figures 1 and 2). Another model [*Mandujano-Velazquez and Keppie*, 2009] suggests that SMC exhumation may be related to subduction of the Tehuantepec ridge system, rapid chain formation (i.e., a 2–2.5 Ma time span) and was relatively unaffected by strike-slip deformation. Consequently, uncertainties about the architecture of the mountain chain include (1) the timing and magnitude of the deformation responsible for exhumation and (2) the role of the PMFS and its eventual transfer of motion to the SMC.

[1]UMR 8217 Géosystèmes, CNRS-Université Lille 1, Villeneuve d'Ascq, France.
[2]Department of Earth and Planetary Sciences, Birkbeck, University of London, London, UK.
[3]Observatoire Midi-Pyrénées, Université Paul Sabatier, GET, Toulouse, France.

Corresponding author: C. Witt, UMR 8217 Géosystèmes, CNRS-Université Lille 1, UFR des Sciences de la Terre, Bâtiment SN5, Avenue Paul Langevin, FR-59655 Villeneuve d'Ascq CEDEX, France. (cesar.witt@univ-lille1.fr)

0278-7407/12/2012TC003141

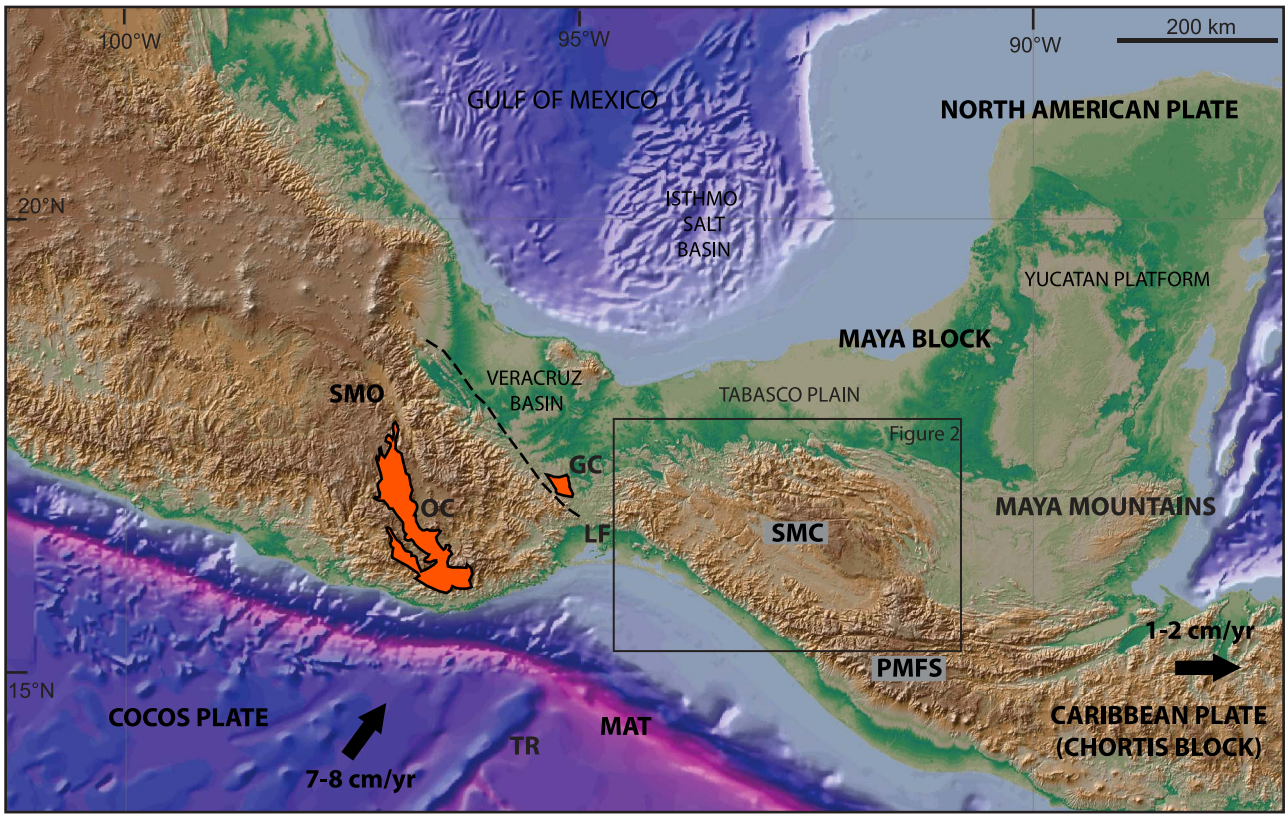

Figure 1. Geodynamic sketch of the triple junction area between the Cocos, Caribbean and North American plates. Plate velocities are from *DeMets et al.* [1990]. Red areas denote ~1 Ga Grenville (Proterozoic) outcrops from *Ortega-Gutiérrez et al.* [1992]. Abbreviations are as follows: GC, Guichicovi complex; LF; Laramide front; MAT, Middle America Trench; OC, Oaxacan complex; PMFS, Polochic-Motagua fault system; SMC, Sierra Madre de Chiapas; SMO, Sierra Madre Oriental; TR, Tehuantepec ridge.

[3] The current position of the triple junction is not well defined, mainly due to the fact that the North American–Caribbean boundary and its intersection with the Middle America trench is poorly resolved beyond its surface expression (the PMFS [*Guzmán-Speziale et al.*, 1989; *Moran-Zenteno et al.*, 2009]). Recent GPS data show that the westernmost segments of the PMFS may not be active at present [*Lyon-Caen et al.*, 2006; *Franco et al.*, 2009], suggesting that left-lateral motion has probably transferred to the SMC, probably along an area coincident with the Sierra de Cuchumatanes [*Witt et al.*, 2012] (Figure 2). Tectonic and kinematic evidence also suggest that the boundary between the North American and Caribbean plates is currently located within the SMC. Seismological and borehole elongation data show that the horizontal component of deformation along the plate boundary currently takes place along the strike-slip faults of the SMC [*Guzmán-Speziale et al.*, 1989; *Guzmán-Speziale and Meneses-Rocha*, 2000; *Witt et al.*, 2012]. In addition, *Andreani et al.* [2008a, 2008b] defined a rigid crustal block (the so-called South Mexico Block), which is bound to the north by the strike-slip faults of the SMC and which migrates to the ESE at ~1 cm/yr. Defining the structural architecture and evolution of the SMC in relation to subduction, the triple junction and the Chortis block migration (i.e., northernmost element of the Caribbean plate, currently moving to the east at circa 1–2 cm/yr [i.e., *DeMets et al.*, 1990; *Lyon-Caen et al.*, 2006; *Franco et al.*, 2009]) are central to resolve this ongoing debate.

[4] Although several studies have proposed different scenarios for Chortis block migration most (reviewed by *Moran-Zenteno et al.* [2009]) can be classified into two major models: (1) The traditional model, which places the Chortis block adjacent to south Mexico near the Xolapa complex prior to its southward migration [*Pindell et al.*, 2006; *Rogers et al.*, 2007; *Ratschbacher et al.*, 2009], and (2) the Pacific model, which place the Chortis block west of its current position [*Keppie and Moran-Zenteno*, 2005]. As more data have become available, it has become clear that there is a strong lithological similarity between the Xolapa complex and the northern part of the Chortis block, with a breakaway period constrained at about 40–45 Ma [*Ratschbacher et al.*, 2009], coincident with the formation of the Cayman trough and the expected onset of the transcurrent motion between the North American and Caribbean plates [*Rosencrantz and Sclater*, 1986; *Leroy et al.*, 2000]. This has led to the traditional model gaining greater acceptance. However, the traditional model fails to account for the absence of significant deformation in the Tehuantepec area, the region now located between the Tonala shear zone (seaward border of the SMC; Figure 2) and the Middle America trench (i.e., the Tehuantepec terrane of *Pindell and Kennan* [2009]). To reconcile

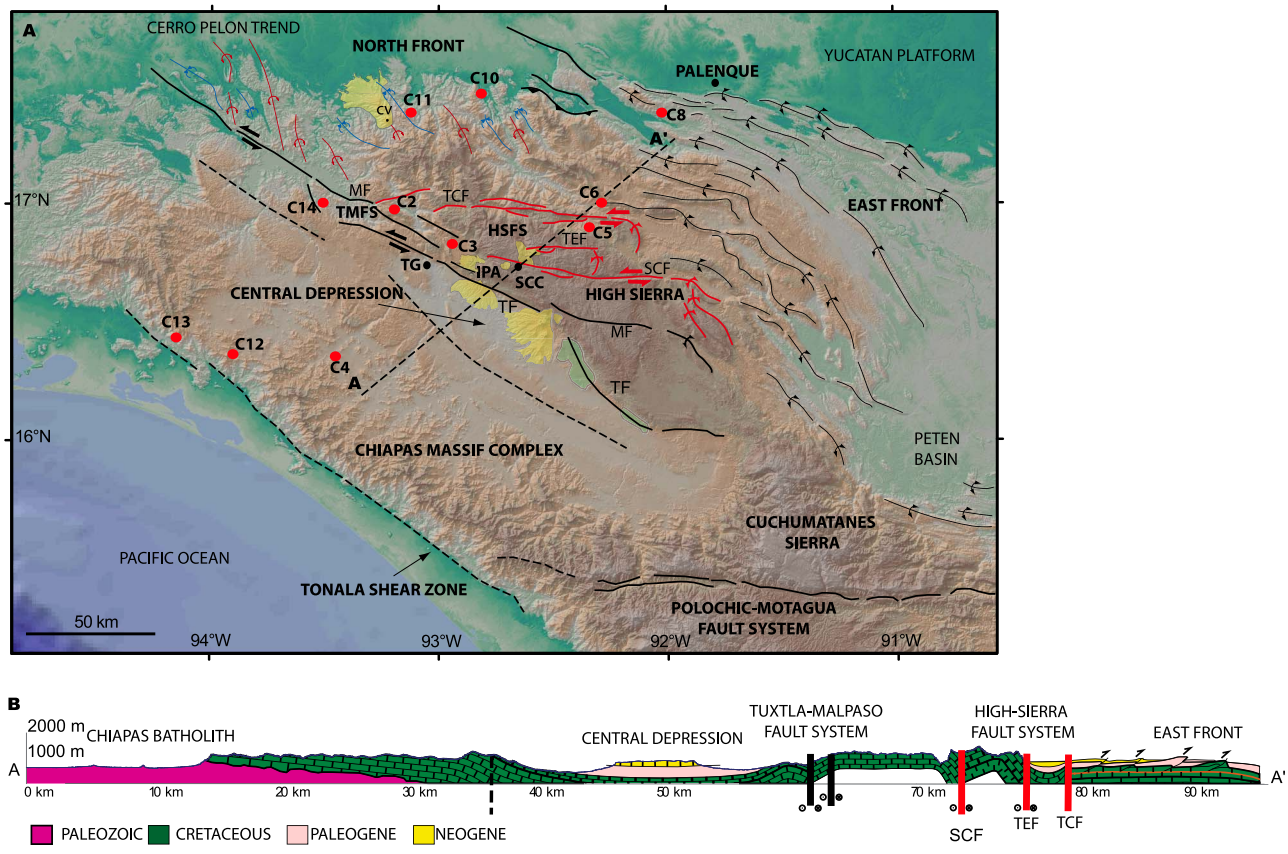

Figure 2. (a) SRTM-derived topography showing the main physiographic zones of the Sierra Madre de Chiapas and surrounding areas. Structural analysis is from *Witt et al.* [2012]. Black strike slip faults show the Tuxtla-Malpaso fault system whereas red strike-slip faults show the High Sierra fault system. Dashed lines correspond to faults showing no current activity. Red circles show collected samples. Black circles show main localities. (b) Schematic cross section showing main lithotectonic units of the chain. Abbreviations are as follows: CV, Chichon volcano; HSFS, High Sierra fault system; IPA, Ixtapa pull-apart basin; MF, Malpaso fault; SCC, San Cristobal de las Casas; SCF, San Cristobal fault; TG, Tuxtla-Gutierrez; TF, Tuxtla fault; TCF, Tectapan fault; TEF, Tenejapa fault; TMFS, Tuxtla-Malpaso fault system.

this, two recent models redefined some aspects of the traditional model and proposed that the transfer zone may have passed seaward from the location of the Tehuantepec block [i.e., *Pindell and Kennan*, 2009] or inland [*Authemayou et al.*, 2011], although the Tonala shear zone is considered as the major transfer zone in some other models [*Wawrzyniec et al.*, 2005; *Ratschbacher et al.*, 2009].

[5] Key questions that need to be addressed include (1) the timing and magnitude of deformation responsible for the formation of the SMC and its present-day topography and (2) the role of the PMFS and thus its connection (if any) to formation of the SMC. To help address these questions this study applied a combination of structural observations, sediment provenance studies (based on detrital zircon U-Pb dating) and apatite thermochronometry (fission track and U-Th-He) to constrain the rock uplift and denudation history of the area. Previous thermochronometry studies in the region were focused mainly on the recent exhumation history of the Chiapas massif complex (CMC) located at the western borders of the SMC [*Ratschbacher et al.*, 2009]. They proposed that CMC construction occurred during two major pulses of deformation at 35–25 Ma and at 12–9 Ma. Supporting evidence should be found in the adjacent Cenozoic sedimentary basins, as they should contain a more complete record of the uplift and denudation history of the SMC and surrounding region, but so far these archives have not been studied. This is unfortunate since a number of previous studies [*Quezada-Muñeton*, 1987; *Carfantan*, 1986; *Gonzáles-Lara*, 2001; *Meneses-Rocha*, 2001] have used the timing of abrupt changes in basin stratigraphy to infer tectonic pulses associated with the growth of the mountain belt. Such links need to be validated and unrelated changes in sediment routing and provenance ruled out. These are the goals of this study.

2. The Sierra Madre de Chiapas

[6] The Sierra Madre de Chiapas (SMC) is part of the Maya block [*Dengo*, 1969], which comprises the SMC, the Yucatan platform and the Maya mountains. Within the SMC it is possible to define, from south to north, six principal structural units showing different lithologies and topographic and/or tectonic architectures (Figure 2): (1) the Chiapas massif complex (CMC); (2) the Central Depression; (3) the High Sierra;

(4) the East Front; (5) the North Front, and (6) the Tabasco coastal plain (i.e., southern Gulf of Mexico). For convenience, units 3 to 5 are grouped and classed as the Chiapas fold-and-thrust belt (i.e., Chiapas Sierra of *Witt et al.* [2012]).

[7] The CMC mostly consists of Permian igneous (mainly granitoid) rocks, most of which are foliated, strongly deformed and metamorphosed [*Weber et al.*, 2007]. The CMC developed from an active continental margin in the early Permian and involved widespread granitic intrusion into a Paleozoic metasedimentary sequence (mainly protholiths correlative with the Santa Rosa, Candelaria and Jocote Formations [*Weber et al.*, 2008; *Estrada-Carmona et al.*, 2009]). The CMC include as well some Ordovician granitoids [*Weber et al.*, 2008]. These rocks were later (252–254 Ma) affected by medium- to high-grade metamorphism [*Weber et al.*, 2007].

[8] *Weber et al.* [2007, 2008] interpreted U-Pb-derived lower intercepts at 258.4 ± 1.9 Ma and 250.9 ± 2.3 Ma as either igneous crystallization or metamorphic ages, and sedimentary protholiths with two principal age distribution peaking at 500–650 Ma and at 1.0–1.2 Ga. Permian basement outcrops are not identified north of the Central Depression; however unpublished drill data from hydrocarbon exploration (Petroleos Mexicanos, PEMEX) have shown that the Permian basement extends to the north into the Tabasco plain and probably into most of the Yucatan platform. The western limit of the outcropping section of Permian rocks at the SMC is coincident with the Tonala shear zone [*Wawrzyniec*, 2005, Figure 2]. An extensive pulse of early middle Jurassic arc magmatism has been defined for igneous rocks overlying and intruding the CMC [*Godínez-Urban et al.*, 2011]. Jurassic (Callovian) red beds and salt deposits overlie these rocks and are partly synchronous with the main pulse of rifting and opening of the Gulf of Mexico [*Carfantan*, 1986; *Pindell et al.*, 2000; *Meneses-Rocha*, 2001], coeval with major rotation of the CMC [*Molina-Garza et al.*, 1992]. Thickness variations of the early Jurassic section have been related to a graben-type geometry derived from the extensional processes associated with opening of the Gulf of Mexico [*Carfantan*, 1986; *Meneses-Rocha*, 2001]. Callovian salt deposits have been recorded as far south as the Central Depression and the Ixtapa pull-apart basin (Figure 2), suggesting that these deposits are widespread beneath the mountain chain.

[9] Most of the Cretaceous stratigraphy corresponds to limestones and dolomites formed in a marine platform setting during the postrift (thermal subsidence) stage of the Gulf of Mexico rift [*Meneses-Rocha*, 2001]. During the Cenozoic sedimentation changes from marine to continental conditions. Paleogeographic reconstructions for the late Cretaceous to early Cenozoic show submerged areas to the north and terrestrial areas to the south [*Carfantan*, 1986; *Meneses-Rocha*, 2001; *Witt et al.*, 2012]. The Paleocene marks the final transition to regional terrigenous sedimentation with deposition of shallow water platform sediments, slope turbidites and deep basinal deposits that outcrop in the northern sections of the SMC (Figure 3). Eocene-Oligocene units consist of continental clastic and minor shallow water deposits in some cases locally associated with carbonate platforms. Oligocene and Miocene units record a marked increase in continental sedimentation, which has been linked to uplift of the CMC (Figure 3) [*Carfantan*, 1986; *Meneses-Rocha*, 2001]. Some igneous activity is also evident: (1) middle-late Miocene intrusions within the Permian basement; (2) subduction-related Plio-Quaternary volcanism in a zone bounding the Central Depression and the High Sierra; and (3) recent volcanism related to the El Chichon volcano along the North Deformational Front [*García-Palomo et al.*, 2004; *Mora et al.*, 2007]. From the middle-late Miocene volcanism migrated inland from the CMC toward the Chiapas fold-and-thrust belt.

[10] Main topographic growth is considered middle-late Miocene in age, defined by fault activity, major stratigraphic unconformities along the SMC and the Tabasco coastal plain, folding at both the eastern and northern fronts, by major salt-related mobility and by the northward progradation of sediments implying the northward migration of the North Front [*Chavez-Valois et al.*, 2009; *Witt et al.*, 2012]. Shortening has been calculated to between 70 and 106 km [*Mandujano-Velazquez and Keppie*, 2009; *Pindell and Kennan*, 2009]. Although, most authors propose that the middle-late Miocene represents the main period of topographic growth of the SMC they differ in the number (from 1 to 6) and timing of tectonic phases and driving processes for mountain belt formation [*Quezada-Muñeton*, 1987; *Carfantan*, 1986; *Gonzáles-Lara*, 2001; *Meneses-Rocha*, 2001]. Most of the proposed growth phases have been linked to abrupt changes in the stratigraphy. For example proposed late Cretaceous to Eocene tectonic pulses have been related to the Laramide orogeny (main tectonic phase leading to the construction of the Sierra Madre Oriental [*Nieto-Samaniego et al.*, 2006] (Figure 1), although the geometry and the tectonic aspects controlling this process remain speculative.

[11] The strike-slip faulting appears to be the main process controlling topographic growth but exactly how is unclear. The only work that sought to explain deformation associated with the strike-slip faulting is a study by *Guzmán-Speziale and Meneses-Rocha* [2000]. These authors proposed that strike-slip motion from the PMFS is transmitted to the SMC as a "fault jog" system. Strike-slip faulting may have accommodated up to 70 km of left-lateral displacement [*Meneses-Rocha*, 2001] with up to 43 km accommodated during the last 6–5 Ma [*Witt et al.*, 2012]. The high-degree of linearity and magnitude of extension (50 to 250 km) of all the major strike-slip faults within the SMC suggest that they are crustal-scale faults (Figure 2). In some cases the narrowness of the deformational area and the poor quality of outcrops prevents a clear geometric and chronologic characterization of fault-related deformation. Major strike-slip faulting occurs mainly to the east of the Central Depression (Figure 2).

[12] In detail, two major systems, comprising five major left-lateral strike-slip faults, appear to control the deformation.

[13] 1. The Tuxtla-Malpaso fault system, a left-lateral strike-slip system that bounds the Chiapas fold-and-thrust belt to the west, is the most prominent tectonic feature of the entire SMC. Greater deformation coincides with the Cerro Pelon trend, a group of folds in an echelon array at the northernmost section of the Tuxtla-Malpaso fault system (Figure 2).

[14] 2. The High Sierra fault system is a dominantly E-W system that includes three major faults. These are from south to north, the San Cristobal, Tenejapa and Tectapan faults. The High Sierra fault system enters into the confined intraplate strike-slip fault category [*Storti et al.*, 2003], due to their rotational or contractional terminations. By contrast, the Tuxtla-Malpaso fault system shows characteristics of

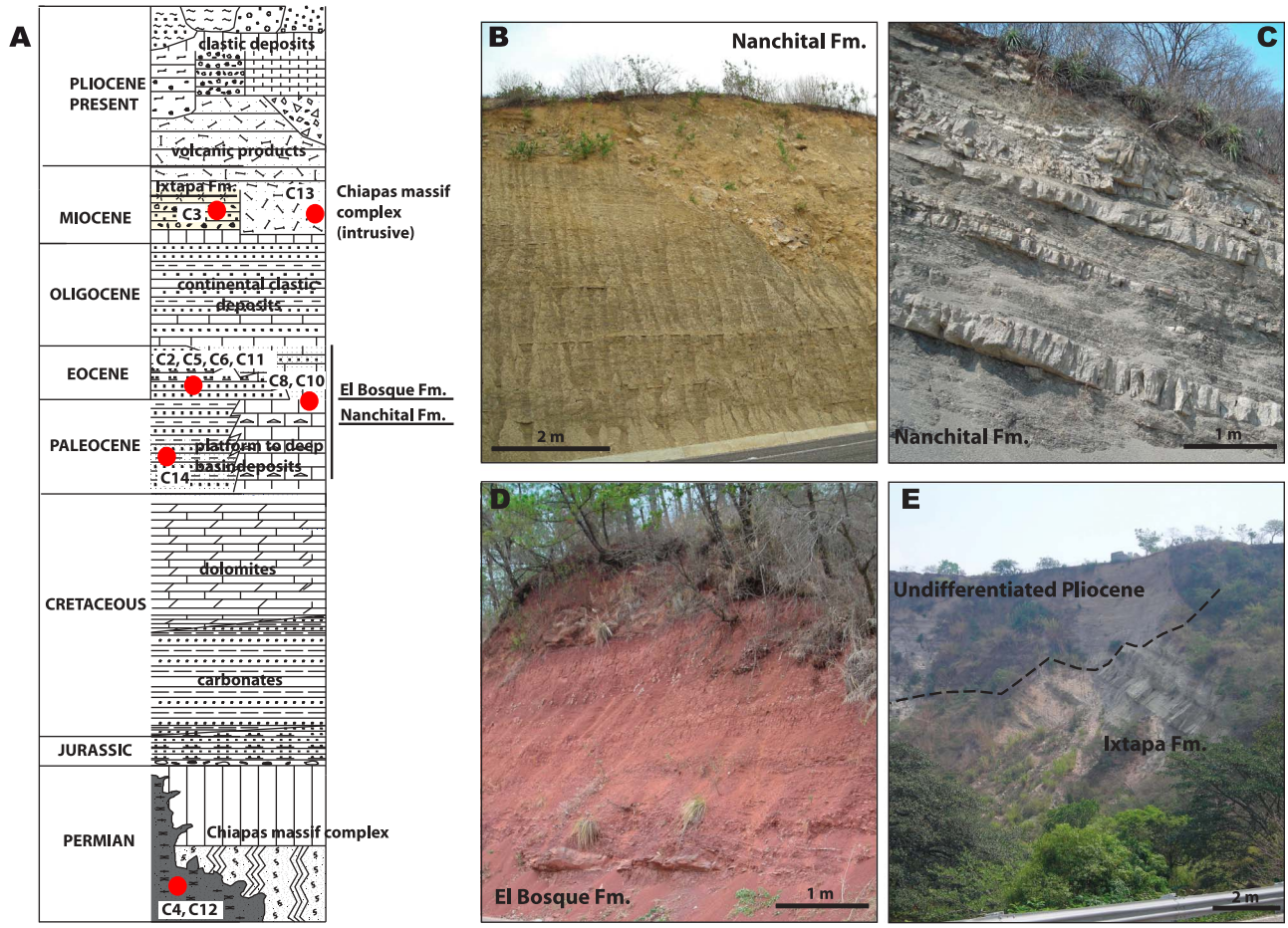

Figure 3. (a) Chronostratigraphic chart of the SMC. Red circles correspond to samples. Formational names are shown for sampled clastic units. Stratigraphic column modified from the 1:200,000 Tuxtla-Gutierrez geological map of the Mexican Geological Survey. (b) Paleocene turbidites at the northern section of the Central Depression. (c) Upper (?) slope turbidite system of the Nanchital Formation. (d) Red thick sandstone and conglomerates of the El Bosque Formation. (e) Main unconformity at the contact between the Miocene Ixtapa Formation and the undifferentiated Pliocene. Locations of samples are shown on Figure 2.

transfer intraplate strike-slip faulting, involving more rigid deformation.

3. Methods and Samples

[15] The aim of this work is to constrain the rock uplift history of the CMC, determine the main processes driving the deformation and test the assumptions made in previous studies that changes in sediment stratigraphy relate to growth stages of the SMC. To meet these aims comparison is made between the exhumation histories of the CMC, derived from apatite fission track (AFT) and U-Th-He (AHe) analyses of bedrock samples, and detrital zircon U-Pb ages from the sedimentary rocks.

[16] The purpose of the detrital zircon U-Pb dating is to test if the granites of the CMC sourced the terrigenous series of the SMC which would help define when exhumation and related erosion may have taken place. In general zircon U-Pb ages will reflect the time of zircon growth, which in most cases is the rock crystallization age, although younger growth events can result from metamorphism but this rarely overprints the zircon cores even up to temperatures as high as 750°C. Detrital zircon U-Pb ages (Figure 4) should therefore be representative of the range of crustal anatexis and/or magma differentiation events within the local basement bedrock/sediment source areas [*Carter and Bristow*, 2000].

[17] AHe and AFT ages were obtained from basement and terrigenous samples to define the exhumation history. The temperature sensitivity of these two methods allows a parcel of rock to be tracked as it cooled from temperatures in excess of 100°C down to ~40°C, the exact temperatures dependent upon rate of cooling and apatite composition (and grain size for U-Th-He). In most cases cooling is related to rock uplift and exhumation driven by erosional denudation and/or tectonics For an average geothermal gradient of 30°C/km such temperatures equate to the uppermost 1–4 km of the Earth's crust. In total, nine AFT and six AHe ages were obtained from the CMC and Paleocene to Miocene terrigenous rocks.

[18] Samples of basement were collected from the CMC and sedimentary samples from the Paleocene-Miocene section of the Chiapas fold-and-thrust belt (Figure 2). Igneous samples from the CMC come from its seaward piedmont

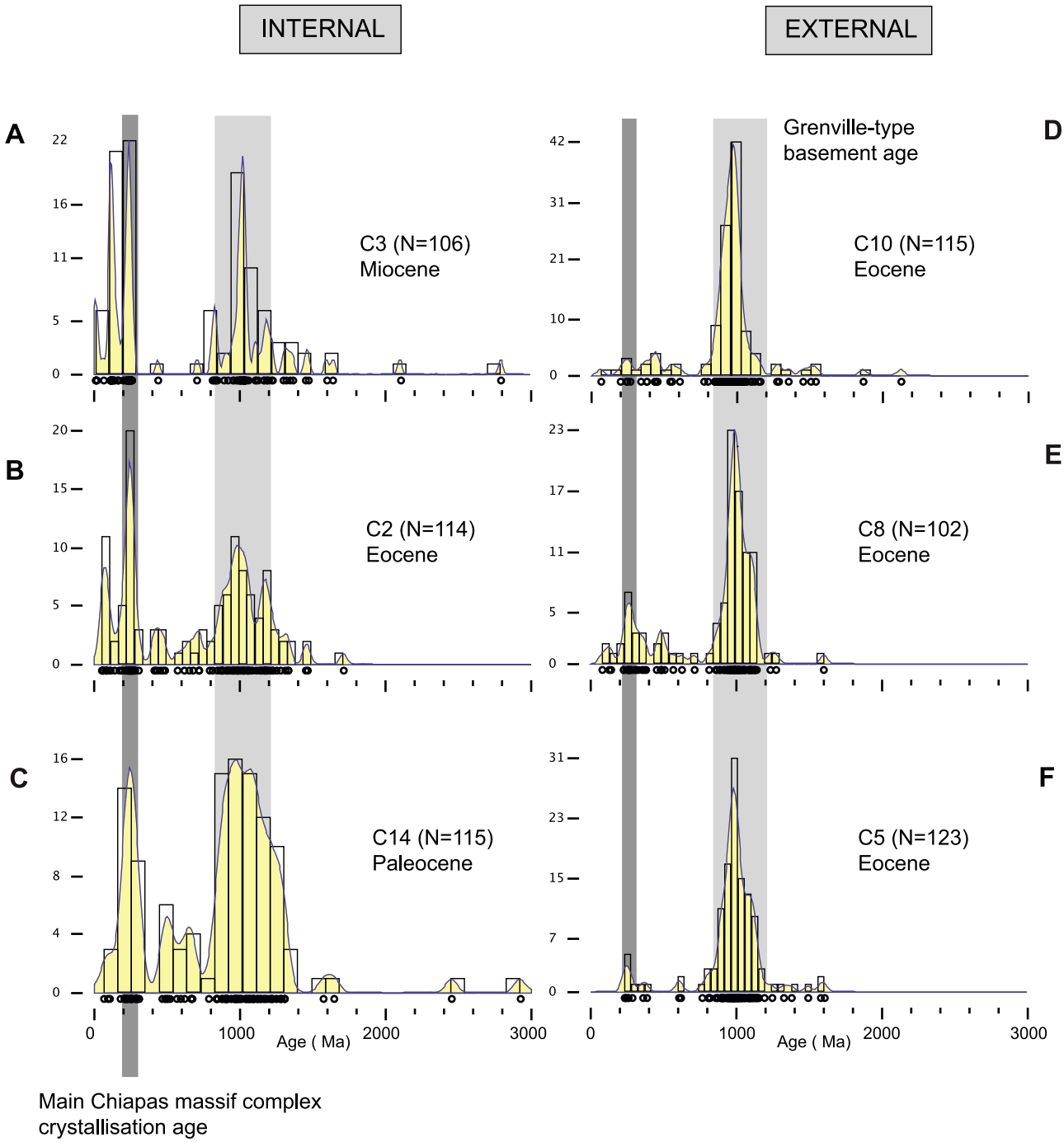

Figure 4. Kernel density plots of detrital zircon ages (<10 discordant) terrigenous samples from the Chiapas Sierra. (a–c) Internal section. (d–f) External section. Light and dark gray rectangles are main Chiapas massif complex (230–270 Ma) and Grenville basement (950–1250 Ma) ages, respectively. See locations of samples in Figure 2. Individual grain ages are provided in the auxiliary material.

(samples C12 and C13) and from its central part (sample C4). Sample C13 corresponds to a granodioritic intrusion. Clastic rock samples of the Chiapas fold-and-thrust belt (Figure 3) are from two different areas that define the internal (C2, C3 and C14) and external (C5, C8, and C10) sections with respect to massif location. These samples are Paleocene-Miocene marine and continental units. The depositional age of the sampled units, from locations where the stratigraphic position is well known is based on the 1:250,000 Tuxtla Gutierrez, Villahermoza, Las Margaritas and Tenosique maps from the Mexican Geological Survey [after *Carfantan*, 1986; *Sanchez-Montes de Oca*, 2006]. Samples C8, C10, and C14 are from turbidite, shallow water and transitional deposits of the Paleocene-Eocene Nanchital Formation (Figure 3). Samples C2, C5 and C6 are from the continental series of the Eocene El Bosque Formation (Figure 3). Sample C3 was

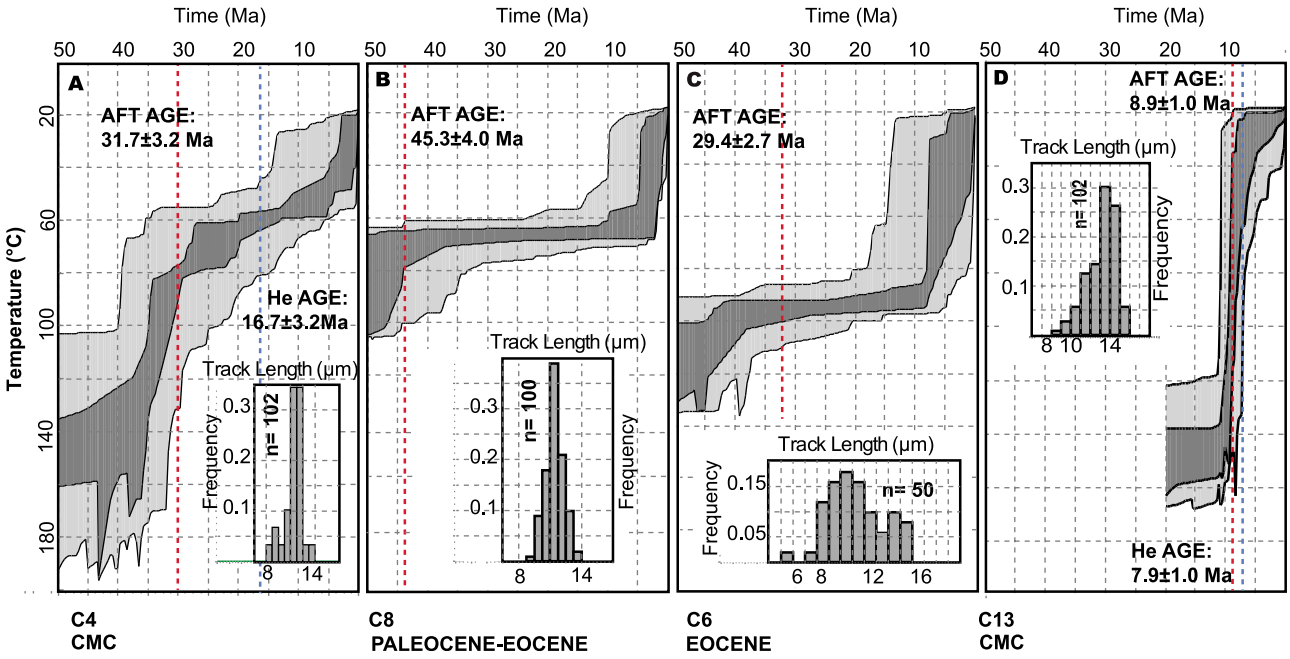

Figure 5. Time-temperature pathways obtained from joint modeling of apatite fission track (AFT) and U-Th-He data. The measured track length distribution is shown for each sample. The red dashed line corresponds to the measured AFT central age. The blue dashed line corresponds to the U-Th-He age. See Figure 2 for the locations of samples. Raw data and methods are given in the auxiliary material.

collected from the Ixtapa Formation, a Miocene continental unit, which outcrops at the northern border of the Ixtapa pull-apart basin. No Oligocene units were analyzed because of the ambiguity of stratigraphic correlations in the field and scarcity of datable zircons and apatite. Sample analyses were conducted at the Thermochronometry Laboratories at the Joint Research School of UCL-Birkbeck, University of London. The methodology and techniques used in this study are detailed in the auxiliary material.[1]

[19] To understand the significance of the AFT and AHe results thermal histories need to be extracted from the data using modeling software that incorporate numerical descriptions of thermal resetting in the FT and U–Th-He systems. For this study, the sample thermal histories were obtained using the modeling package HeFTy of *Ketcham* [2005], which includes the multicompositional AFT annealing algorithm of *Ketcham et al.* [2007]. This software performs inverse modeling of the AFT and AHe data with a Monte Carlo search for better fitting cooling paths through a set of user-defined t–T boxes. Where appropriate AFT and helium ages were modeled jointly and, t–T histories were generated. Because no thermal history ever uniquely defines a set of AFT or AHe data, the better fitting thermal histories must always be considered in the context of local geological constraints. The outputs are thermal histories that predict AFT and AHe parameters that most closely match the measured data. Goodness of fit between predicted and observed parameter distributions was defined by Kuiper's Statistic [*Ketcham*, 2005]. Figure 5 provides a graphic summary of representative modeled thermal histories for different samples across the SMC. For each sample, dark gray shading outlines the cluster of 100 better fitting cooling paths obtained from a larger population of Monte Carlo trials (typically 10^4–10^5). Lighter gray shading outlines the spread within that same population of "acceptable" (i.e., relatively less robust) paths, here defined by a less stringent goodness-of-fit criterion of 0.05. Apatite FT, U-He and zircon U-Pb results are summarized in Table 1, and the raw data are provided in Tables S1 and S1 and Data Set S1 in the auxiliary material.

4. Results and Interpretation

4.1. Zircon U-Pb

[20] The detrital U-Pb data obtained from the six clastic samples yielded >100 grain ages hence sufficient grains ages have been measured to give statistical confidence that the data capture the principal zircon sources [*Vermeesch*, 2004]. The data are displayed as kernel density plots [*Vermeesch*, 2012] in Figure 4. Sedimentary rock samples from the internal section are dominated by ages at ~250 Ma and ~1 Ga, with minor occurrences between 300 and 500 Ma (Figure 4). Paleocene sample (C14) from a turbidite deposit obtained near the Tuxtla-Malpaso fault system area and Eocene sample C2 sample yielded two main age peaks at 200–250 Ma (late Permian) and Proterozoic zircon grains that range from circa 900 to 1400 Ma. Although most have zircons ages at ~1.0–1.05 Ga there is also an important peak around 1.2 Ga. There is also a group of Braziliano-Pan African zircons between ~500 and ~700 Ma and another group of Ordovician zircon grains. Sample C3 contains more Permian and Jurassic zircons (an assemblage typical of the CMC and its sedimentary cover, i.e., the Todos Santos Formation) and an additional group of Miocene zircon grains ranging from 20 to

[1]Auxiliary materials are available in the HTML. doi:10.1029/2012TC003141.

Table 1. Summary of Sample Locations and Apatite Fission Track, U-Th-He and U-Pb Results

Sample	Sample Location	Altitude (m Above Sea Level)	Rock Unit and Age	AFT Age (Ma ± 1σ)	Mean Track Length (μm)	Corrected AHe Age (Ma ± 1σ)	Main U-Pb Age Peaks
			Basement Samples				
C4	16°24′04″N; 93°04′55″W	680	Permian batholith	31.7 ± 3.2 (n = 14)	12.43 ± 0.17 (n = 102)	16.7 ± 3.2 (n = 3)	-
C12	16°20′41″N; 93°52′26″W	655	Permian batholith	9.6 ± 0.8 (n = 22)	13.55 ± 0.16 (n = 100)	-	-
C13	16°24′55″N; 94°7′3″W	465	Miocene intrusion	8.9 ± 1.0 (n = 19)	14.14 ± 0.16 (n = 102)	7.9 ± 1.0 (n = 2)	
			Sedimentary Samples				
C2	17°0′6″N; 93°9′1″W	440	Eocene	-	-	5.6 ± 2 (n = 4)	∼250 Ma; 0.8–1.2 Ga (n = 114)
C3	16°50′31″N; 92°54′11″W	1100	Miocene	40.3 ± 5.4 (n = 7)	12.05 ± 0.91 (n = 2)	-	∼250 Ma; 0.8–1.2 Ga (n = 106)
C5	16°54′37″N; 92°20′44″W	1150	Eocene	-	-	-	0.8–1.2 Ga (n = 123)
C6	16°59′33″N; 92°18′7″W	1150	Eocene	29.4 ± 2.7 (n = 15)	11.25 ± 0.34 (n = 50)		-
C8	17°24′10″N; 91°59′25″W	340	Eocene	45.3 ± 4.0 (n = 12)	12.6 ± 0.15 (n = 100)	-	∼250 Ma; 0.8–1.2 Ga (n = 102)
C10	17°27′32″N; 92°46′59″W	100	Eocene	11.4 ± 2.2 (n = 8)	11.59 ± 0.71 (n = 4)	3.4 ± 1.2 (n = 5)	0.8–1.2 Ga (n = 115)
C11	17°24′10″N; 93°6′3″W	330	Eocene	8.9 ± 1.5 (n = 13)	12.93 ± 0.68 (n = 3)	1.5 ± 1.0 (n = 3)	-
C14	17°1′46″N; 93°31′59″W	360	Paleocene	16.5 ± 2.1 (n = 16)	13.66 ± 0.34 (n = 31)	5.4 ± 0.8 (n-4)	∼250 Ma; 0.8–1.2 Ga (n = 115)

17 Ma, suggesting igneous, probably volcanic activity during the Miocene.

[21] Three terrestrial to shallow marine Paleocene-Eocene sedimentary samples from the external section have zircons with ages up to 1.2 Ga with minor numbers of Permian, Jurassic or Brazilio–Pan African grain ages. Although zircon ages in samples C5, C8 and C10 cluster at ∼1 Ga there are also zircons with ages up to 1.2 Ga, typical of Oaxaquia and a few isolated grains with ages between at 1.3–1.5 Ga. As these are rare it is likely they come from inherited cores.

4.2. Apatite Fission Track and U-Th-He

[22] The quality of the apatite fission track data is mixed, affected by grain type (inclusions, zoning, defects) and low abundances. Table 1 summarizes the results for the nine AFT samples of which six yielded adequate numbers of track lengths and single-grain ages suitable for thermal history modeling. There is no evidence of extra (non-Poisson) dispersion among the single-grain data; hence, apatite grain composition has not led to variable annealing within each sample. AHe dating was performed on six samples (bedrock and clastic) and involved between 3 and 5 replicates per sample. Age reproducibility was very good, and only one replicate had to be rejected (sample C13; see auxiliary material) due to an anomalously high age, most likely caused by inclusions or implantation.

[23] AFT and U-Th-He cooling ages obtained at the SMC belong to three main age ranges (Table 1): (1) 45.3 ± 4.0 to 29.4 ± 2.7 Ma ages found across the whole study area; (2) 16.5 ± 2.1 to 8.9 ± 1.5 Ma ages confined to CMC and terrigenous rocks of the High Sierra and the North Front, and (3) ages between 5.6 ± 2.0 and 1.5 ± 1.0 Ma from areas close to the Tuxtla-Malpaso fault system and from the North Front (Figure 2).

[24] AFT data obtained from the east section of the CMC (sample C4) record an age of 31.7 ± 3.2 Ma with an AHe age of 16.7 ± 3.2 Ma. Track lengths are unimodal with a mean of 12.43 ± 0.17 μm. Time-temperature history obtained from modeling shows relatively constant exhumation since ∼30 Ma with a small rise from ∼10–7 Ma (Figure 5a). Samples C12 and C13 are from the external zone of the massif (Tonala shear zone). The Permian sample C12 displays an AFT age of 9.6 ± 0.8 Ma whereas sample C13 (granodioritic intrusion) yielded similar ages 8.9 ± 1.0 Ma (AFT) and 7.9 ± 1.0 Ma (AHe) diagnostic of rapid cooling to surface or near surface temperatures.

[25] A Paleocene terrigenous sample of the internal section (sample C14) yielded an AFT cooling age of 16.5 ± 2.1 Ma with a mean track length of 13.66 ± 0.34, consistent with relatively fast cooling, although only 31 tracks lengths were measured. AHe ages of 5.6 ± 2 and 5.4 ± 0.8 were obtained from samples C2 and C14, which are from areas under the influence of the Tuxtla-Malpaso fault system. Numbers of measured confined fission tracks were not sufficient to model a T-t history. The 40.3 ± 5.4 Ma AFT obtained from C3 sample is older than the age of deposition and therefore corresponds to the cooling age of the sediment source area.

[26] Terrigenous samples of the external section yielded six AFT and AHe ages between 45.3 ± 4.0 and 1.5 ± 1 Ma. In all cases the magnitude of post deposition heating has been sufficient to reset the apatites and remove any provenance signal. Thermal histories for the Paleocene-Eocene data (C6 and C8) yielded very similar T-t pathways (Figure 5). In both cases the modeled cooling histories show long intervals of little or no cooling (flat sections in Figures 5b and 5c) consistent with very low rates of exhumation between 30 Ma and 10 Ma. From ∼10–7 Ma cooling rates show a marked increase consistent with rock uplift at this time,. The timing is in agreement with the AFT ages obtained from samples C10 and C11,

which range between 11.4 ± 2.2 to 8.9 ± 1.5 Ma. The North Front shows very young and similar (within errors) AHe ages of 1.5 ± 1 and 3.4 ± 1.2 Ma (samples C11 and C10, respectively).

[27] In summary, thermal history modeling has shown that exhumation during the Eocene-Oligocene was concentrated along the CMC and that the Chiapas fold-and-thrust belt is almost unaffected by this process, supported by very low rates of cooling on the thermal history plots. Cooling rates then show a marked increase in the middle-late Miocene and this appears to have affected the whole chain. It was more rapid along the zones located next to the major strike-slip systems such as the Tonala shear zone or the Tuxtla-Malpaso fault system (sample C14).

5. Discussion

5.1. Basement Sources and Terrigenous Sediments

[28] Detrital zircon dating yielded two main groups of ages: (1) ~0.85–1.2 Ga related to basement rocks affected by the Grenville event (i.e., 950–1250 Ma [*Ortega-Gutiérrez et al.*, 1995; *Weber and Kohler*, 2009]) and (2) 240–270 Ma related to the intrusion of the Permian arc-related granitoids into the CMC (Figure 4). The 0.85–1.2 Ga ages are more abundant to the north (i.e., along the external zone located at the High Sierra, and the North and East Fronts). As many of the dated zircons were euhedral and showed no evidence for Permian overgrowths we interpret the Proterozoic age peak of samples C5, C8 and C10 to record the age of the source rock. These samples are dominated by Grenville basement sources with minor contributions from the Permian batholiths (Figures 4 and 6). The internal and external terrigenous areas show marked differences in sediment provenance. Sedimentary rock samples from the western border of the Chiapas fold-and-thrust belt (internal section) yielded broad age spectra with the main age groups consistent with sources from the CMC (Figures 4 and 6), whereas samples from the external areas are almost entirely defined by Grenville age sources.

[29] Grenville basement outcrops have not been identified in the Maya block. Closest exposure areas are located further north at the Oaxacan block (Figure 6c) and the Guichicovi complex, which have the most extensive outcrop of Grenville basement in the south of Mexico and the triple junction area (Figure 1) [*Ortega-Gutiérrez et al.*, 1992; *Keppie et al.*, 2003; *Weber and Hecht*, 2003; *Ducea et al.*, 2004; *Solari et al.*, 2009]. Grenville zircons have been documented as protoliths in the Chaucus and Chortis complexes [i.e., *Ratschbacher et al.*, 2009, Figure 6d] and in metasediments in many areas north and south of the SMC. The Cuicateco terrane, the Chivillas Formation, the San Diego phyllite, the Sepultura unit, the Todos Santos unit and the Baldy unit are some of the examples of detrital series where Proterozoic ages have been determined (Figures 6e to 6h) [*Ortega-Gutiérrez et al.*, 2007; *Weber et al.*, 2008; *Pérez-Gutiérrez et al.*, 2009; *Martens et al.*, 2010; *Torres de León et al.*, 2012].

[30] The dominance of Grenville sources for sedimentary rocks distributed at the external section of the SMC is hard to reconcile with basement outcrops defined at the CMC and at the Maya block south and east of the Tehuantepec isthmus. There are only traces of ~400 Ma zircons, which are one of the most common basement ages found at the south Maya block and south of the PMFS [*Ratschbacher et al.*, 2009; *Martens et al.*, 2010] (Figure 6a). That such ages are only present at trace levels in the studied samples implies that this was not an important source. There is also a general lack of 500–650 Ma zircons, known to be present as inherited cores in detrital zircons from the CMC (i.e., Santa Rosa Formation [*Weber et al.*, 2008]). Sediment input recognized in the external area section fits with a northern source, most likely related to the Oaxaca Block or the Guichicovi complex; which as previously suggested are the closest Grenville exposure areas. Furthermore, all of the terrigenous samples show age peaks between 950 and 1050 Ma, which spans the Zapotecan tectonothermal event recorded in the Oaxacan complex [*Keppie et al.*, 2003; *Solari et al.*, 2004, 2007]. A northwest provenance of Paleocene to Eocene sediments is also supported by coeval eastward stratigraphic pinch-outs observed on seismic lines next to the North Front [*Witt et al.*, 2012]. Furthermore, *Nieto-Samaniego et al.* [2006] suggest that the Oaxaca Block recorded important Laramide shortening coincident with major erosion during the Paleocene-Eocene (a time span coincident with the sampled sedimentary units). Northward sourced Paleocene to Eocene marine and terrestrial units were deposited in a deep clastic sea and basin margin or transitional continental areas that developed to the north of the Chiapas Sierra (Figure 7). The tectonic context is most likely that of a foreland-type basin related to a Laramide deformation front [*Witt et al.*, 2012]. The amount of sediment input from the Laramide front was sufficient to cause significant burial of the Paleocene-Eocene sediments and resetting of the AFT chronometers, hence minimum depths of burial are 2–3 km based on global average geothermal gradients. Although we favor a northern source for the reasons outlined above, we cannot rule out the possibility that some of the sediment came from the south because Proterozoic zircons are also found in the metasediments of the Baldy unit (Figure 6e) outcropping at the Maya mountains [*Martens et al.*, 2010].

[31] The CMC may not have been the main source of sediments until it experienced enhanced uplift between 16 and 10 Ma (see section 4.2), which postdates the Paleocene-Eocene sedimentary units from which age spectra has been obtained at the North Front. From the Paleocene to Miocene the areas surrounding the Central Depression show a local sediment provenance from the CMC. Further north, Permian massif-related inputs decrease drastically, and in some cases are effectively missing. This is most likely related to low rates of denudation of the massif over this time interval. Furthermore, Braziliano-African zircons (~500 Ma to ~700 Ma such as those of the Santa Rosa or Todos Santos Formations [*Weber et al.*, 2008; *Pérez-Gutiérrez et al.*, 2009] and Ordovician zircons (typical of intrusions at the CMC and at most of the Maya block [*Weber et al.*, 2008; *Martens et al.*, 2010]) are present in the internal section but missing at the external one. Although, the CMC may have locally sourced the internal section of the SMC during Paleocene-Eocene, our detrital zircon U-Pb results suggest that the CMC did not become the main sediment source (and therefore was not subject to major surface uplift) until the onset of the major tectonic deformation during middle-late Miocene (see section 5.2).

5.2. Exhumation Age and Processes

[32] To see if there is any regional pattern to exhumation, AFT ages from *Ratschbacher et al.* [2009] were plotted

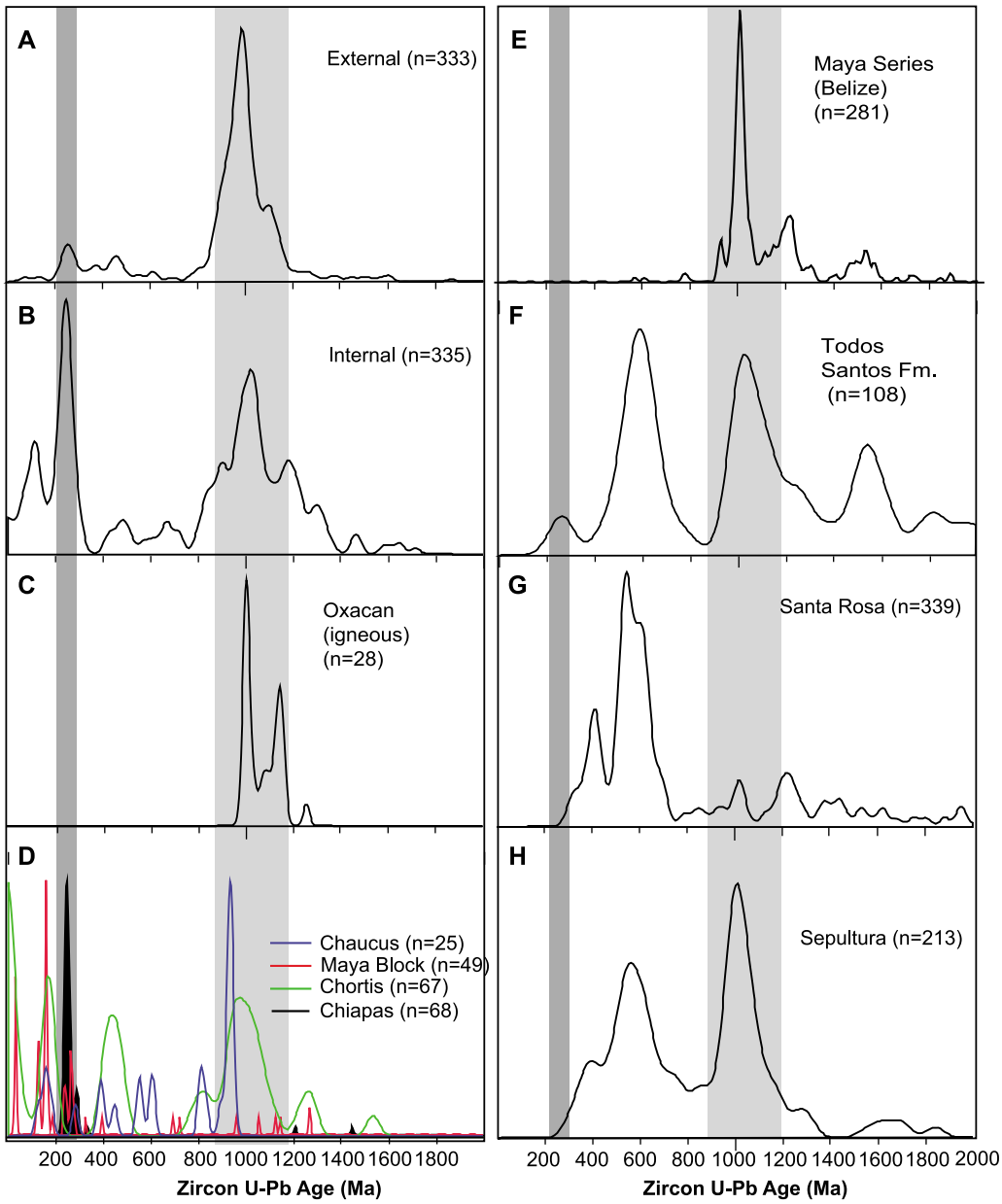

Figure 6. (a and b) Kernel density plots of detrital zircon U-Pb ages from the terrigenous (external and internal) sections of the chain. (c–h) Kernel density plots for igneous and metasedimentary rocks outcropping in south Mexico, Belize and Guatemala. Original reference for plots are as follows: Figure 6c from *Keppie et al.* [2003]; Figure 6d from *Ratschbacher et al.* [2009]; Figure 6e from *Martens et al.* [2010]; Figure 6f from *Perez-Gutierrez et al.* [2009]; Figures 6g and 6h from *Weber et al.* [2008].

against sample elevation together with the new data from this study (Figure 8). The middle-late Eocene cluster of the older ages point to onset of exhumation at or before this time but the preservation of these old ages, which are mostly found at the highest elevations, and the results from thermal history modeling (Figures 5 and 8) show that exhumation rates were relatively low at this time. Ages in the range from 39 to 25 Ma documented by *Ratschbacher et al.* [2009] from the inner (seaward) southern section (i.e., Mexico-Guatemala border area) of the massif did not yield clear age/elevation trends and have been interpreted as rapid cooling at ~30 Ma. Similarly, the Chuacús complex (north of the Motagua fault zone) and the Las Ovejas complex (south of the Motagua fault) show AFT clusters ranging from ~25 Ma to ~35 Ma [*Ratschbacher et al.*, 2009].

[33] The Eocene-Oligocene period coincided with the onset of major clastic sedimentation along the Chiapas Sierra and has been related to SMC exhumation during the Laramide tectonic phase [*Carfantan*, 1986; *Meneses-Rocha*, 2001] or to the onset of migration of the Chortis block [*Ratschbacher et al.*, 2009]. Thermal histories of samples from the North and East Fronts do not record any exhumation

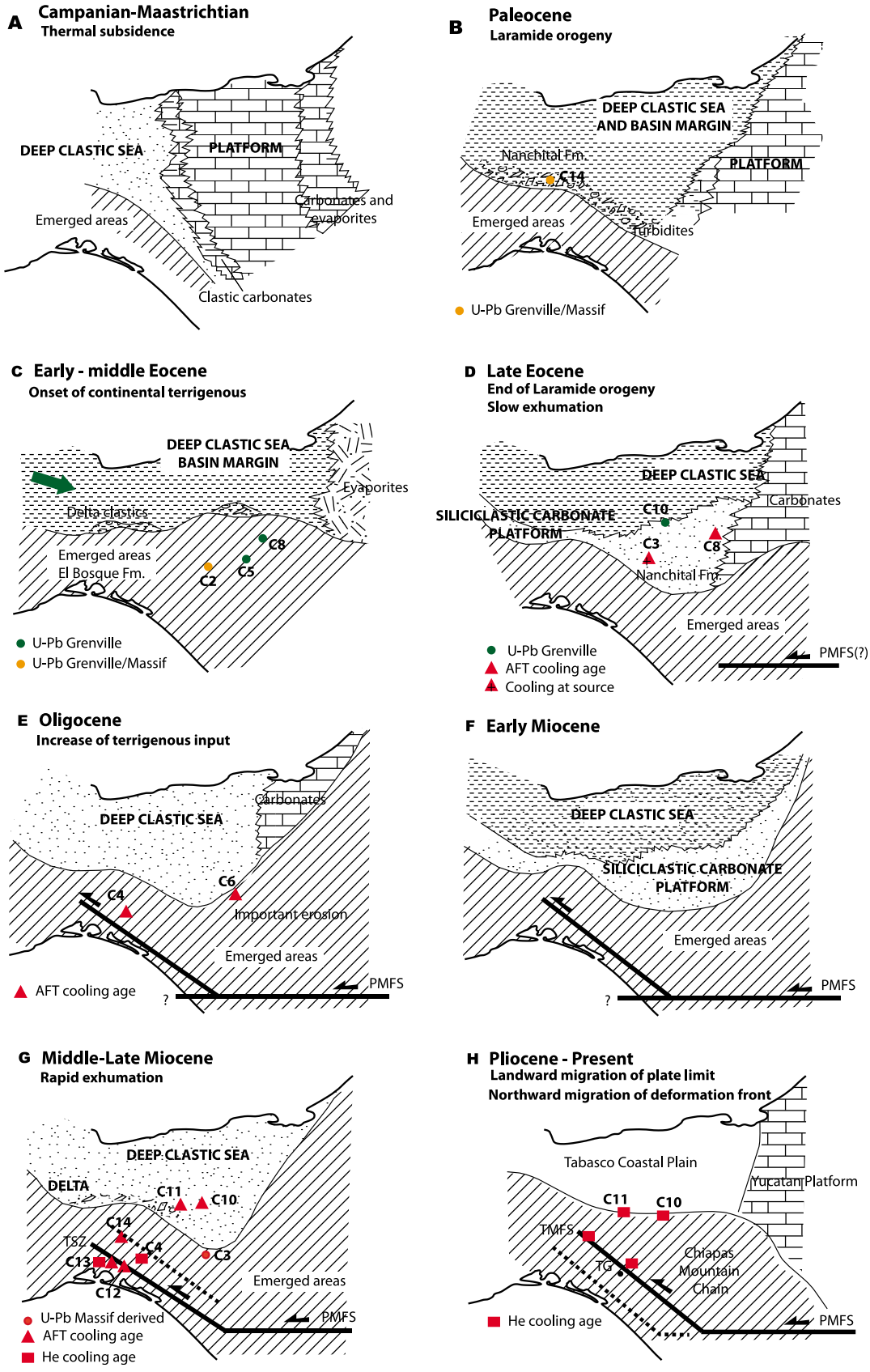

Figure 7. Paleogeographic reconstructions based on the works by *Carfantan* [1986], *Meneses-Rocha* [2001] and *Witt et al.* [2012], which include, for each period, any constraints from the detrital zircon provenance and thermochronological data obtained by this study.

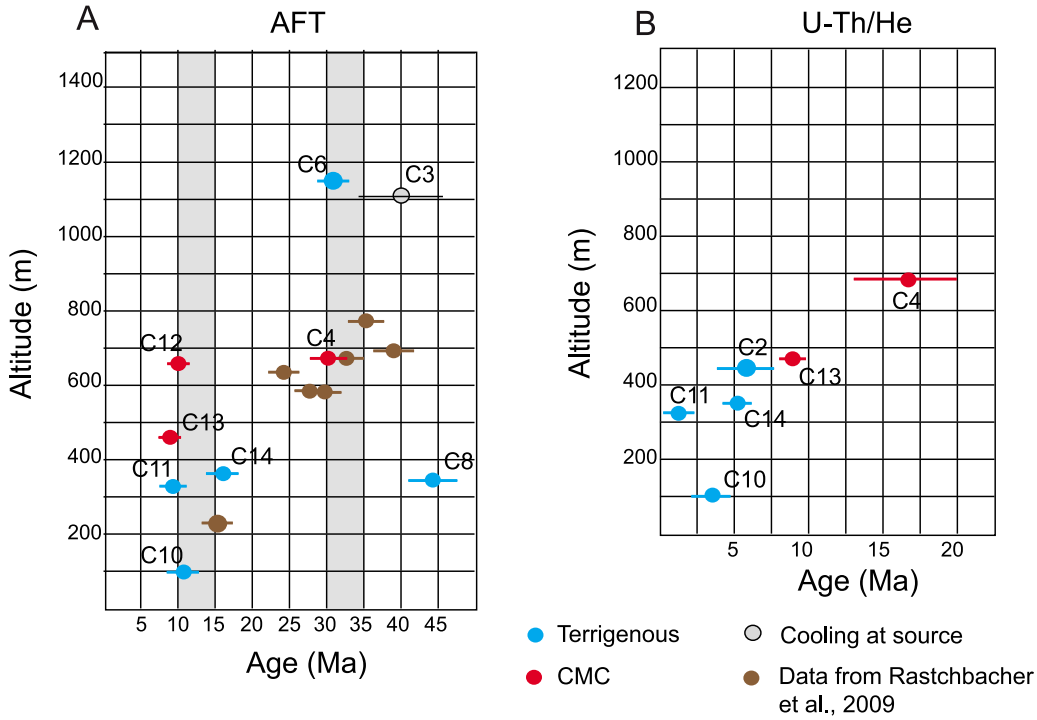

Figure 8. (a) Summary of AFT results obtained in this work and from *Ratschbacher et al.* [2009]. Gray boxes define major clustering of AFT ages. (b) U-Th/He obtained in this study.

during Eocene-Oligocene times showing that the Chiapas fold-and-thrust belt was relatively unaffected by the deformation. As suggested by *Quezada-Muñeton* [1987] and observed in the field within the Chiapas fold-and-thrust belt there are no tectonic-related unconformities in the sedimentary sequence spanning the Paleocene to late Miocene. The AFT-derived thermal histories are consistent with this. Thus the Chiapas fold-and-thrust belt did not experience any significant uplift during the Eocene-Oligocene.

[34] The youngest AFT ages in Figure 8a occur at lower elevations and are the same (within error) over a 600 m elevation range consistent with more recent and rapid uplift. Late Miocene (10–9 Ma) cooling ages for the massif have been associated with near-field left-lateral shearing and volcanism along the areas close to the faults related to the PMFS and the Tonala Shear Zone [*Ratschbacher et al.*, 2009]. Furthermore, these authors suggest that the 10–9 Ma shear event defines the location of the limit between the Caribbean and North American plates at this time, with the transpressive deformation resulting from a major change in the trend of the PMFS relative to the Tonala shear zone. However, our data show that this event was more regional in extent. For example, the North Front records uplift between 11.4 ± 2.2 Ma and 8.9 ± 1.5 Ma. AFT-derived thermal histories obtained from terrigenous samples of the High Sierra and East Front show a similar onset of high rates of cooling from ~10 to 7 Ma.

[35] The Tuxtla-Malpaso fault system (Figure 2) is the most prominent tectonic feature of the entire SMC. Two AHe ages record exhumation at the Tuxtla-Malpaso fault system at 5.6 ± 2 Ma and 5.4 ± 0.8 Ma. This is in agreement with major syntectonic sedimentation occurring from 6 to 5 Ma onward with major depocenters developing at the transtensional Ixtapa pull-apart basin and at the transpressional Cerro Pelon trend (Figure 2) [*Meneses-Rocha*, 2001; *Witt et al.*, 2012]. Horizontal displacement along the northern section of the Tuxtla-Malpaso fault system could have thus reached ~30 to 40 km during the last 6–5 Ma involving 0.5 to 0.8 cm/a^{-1} of lateral accommodation [*Witt et al.*, 2012]. This rate accounts for a great part of the current relative motion between the Caribbean and North American plates that may be transmitted to the SMC area, as it has been constrained by GPS and kinematic models [*Lyon-Caen et al.*, 2006; *Andreani et al.*, 2008a, 2008b].

[36] Thermochronologic and tectonic observations suggest that the strike-slip deformation along the margins of the Caribbean and North American plates jumped from the Tonala Shear Zone to the Tuxtla-Malpaso fault system between 10 and 5 Ma, and most likely from 6 to 5 Ma as evidenced by the AHe obtained for this study. An eastward migration of deformation from the Tonala Shear Zone to the Tuxtla-Malpaso fault system is in agreement with depocenter evolution [*Meneses-Rocha*, 2001], strain and seismicity observations [*Guzmán-Speziale and Meneses-Rocha*, 2000], GPS-derived data [*Lyon-Caen et al.*, 2006], kinematic models [*Andreani et al.*, 2008a, 2008b; *Authemayou et al.*, 2011] and the migration of volcanic products [*Mora et al.*, 2007].

5.3. The Chiapas Area and the Triple Junction

[37] There is growing evidence to suggest that the strike-slip regime between the Caribbean and North American plates is currently located within the SMC [*Guzmán-Speziale and Meneses-Rocha*, 2000; *Lyon-Caen et al.*, 2006; *Andreani et al.*, 2008b; *Franco et al.*, 2009; *Witt et al.*, 2012]. These include GPS constraints that suggest that the westernmost

section of the PMFS is currently inactive and that lateral motion may have been transmitted to the SMC [*Lyon-Caen et al.*, 2006; *Franco et al.*, 2009], and new kinematic models that show the SMC corresponds to a crustal restraining bend resulting from the action of a major left-lateral structure connecting the PMFS to the south to the strike-slip systems of the SMC to the north [*Andreani et al.*, 2008b]. The new thermochronologic evidence described here also strongly supports the migration of the transpressional deformation landward from the Tonala shear zone to the Tuxtla-Malpaso fault system between 10 and 5 Ma. Similarly, Neogene morphological markers seem to show a migration of deformation from the Motagua to the Polochic Fault in northern Guatemala over the same period of time [*Authemayou et al.*, 2011]. Indeed, extension related to activity of the PMFS has been propagating northward since the late Miocene making the triple junction diffuse as it migrates eastward and inland within the continental crust [*Authemayou et al.*, 2011].

[38] Our data do not cover the entire CMC preventing detailed examination of exhumation in the wake of the migrating Chortis block. However, several aspects may be considered. The 30–25 Ma exhumation period defined here is coincident with the arrival of the Chortis block to the Tehuantepec area and as proposed by previous studies [e.g., *Ratschbacher et al.*, 2009] this exhumation period may be strongly related to the effects of Chortis. In this scenario the CMC, located closer to the Tehuantepec area was uplifted whereas the Chiapas fold-and-thrust belt did not record major exhumation at that time. The relative quiescence between ~30 Ma and ~16 Ma may suggest that the entire SMC was far away from the zone affected by Chortis migration. This agrees with models that propose that the Chortis block was located south of the undeformed Tehuantepec block after ~30 Ma [i.e., *Pindell and Kennan*, 2009].

[39] The topographic growth of the SMC including the CMC was related to the transpressional effects of the diffuse triple junction so that the Tonala shear zone may have accommodated significant deformation since 16 Ma [*Witt et al.*, 2012]. But it is unclear whether the marked rise in exhumation between 16 and 9 Ma coincided with the arrival of the Chortis block to the area now occupied by the diffuse triple junction. More exhumation data, especially along-strike, are needed to know whether the thermochronological history recorded by the areas adjacent to the Tonala shear zone, especially the ~10 Ma signal, may or may not have recorded the southward migration of Chortis.

[40] Other regional aspects to consider, and which span the temporal tectonic changes in the SMC include (1) super fast spreading on the East Pacific Rise between 18 and 10 Ma [*Wilson*, 1996]; (2) NE-SW migration of the volcanic arc activity and opening of the Nicaraguan back-arc basin from 10 to 0 Ma [*McIntosh et al.*, 1993]; and (3) subduction of the Tehuantepec ridge [*Mandujano-Velazquez and Keppie*, 2009]. Some of these aspects have been cited by *Mann et al.* [2007] as the plate tectonic processes mostly likely responsible for the current architecture of the triple junction area. Along-strike variation of interplate coupling (Cocos slab) with strong and weak coupling north and south of the PMFS, respectively [*Franco et al.*, 2009], could be considered as a driving factor for formation of the SMC. The middle-late Miocene is also a period of rapid exhumation across south Mexico and the Guatemala-Honduras [*Ratschbacher et al.*, 2009]. Middle-late Miocene compressive deformation has been observed in the Peten Basin, Campeche, the Veracruz Basin, the Tabasco area and the Mexican Ridge [*Jennette et al.*, 2003; *Ambrose et al.*, 2003; *Mitra et al.*, 2005; *Le Roy et al.*, 2008; *Rangin et al.*, 2008; *Alzaga-Ruiz et al.*, 2009; *Witt et al.*, 2012]. Although deformation mechanisms observed in these areas may differ, the middle-late Miocene appears as one of the most prominent periods of deformation across southern Mexico.

6. Conclusions

[41] U-Pb zircon dating has shown that most of the Paleocene to Eocene predeformational sedimentary rocks along the northern section of the Chiapas fold-and-thrust belt were likely sourced from a Grenville age terrain, probably within the Oaxaca Block or the Guichicovi complex, located north of the SMC. Other possible source areas may be related with the Baldi unit outcropping at the Maya mountains. Cenozoic sedimentary rocks that were predominantly sourced from the CMC are concentrated along the internal sections of the Sierra and become significantly more important with the onset of major deformation between 16 and 9 Ma. These results are incompatible with models that have proposed a simple relationship between uplift of the CMC and increase in continental-type sedimentation. We also found that exhumation and erosion along a Laramide front, from the early Paleocene to Eocene, was an important source of sediments for the north section of the SMC. Sediment input and related burial at this time was sufficient to reset the AFT chronometers.

[42] No evidence for significant regional erosion was found at the Chiapas fold-and-thrust belt for the Eocene-Oligocene (a period probably coincident with the onset of regional transpression associated with the initiation of motion along the PMFS). The CMC saw modest erosion whereas the Chiapas fold-and-thrust belt seems to have experienced little or no erosion as expressed by flat time-temperature histories between 30 and 16–9 Ma. This is in agreement with the absence of tectonic-related unconformities along the Chiapas fold-and-thrust belt and with previous thermochronological records obtained at the massif [*Ratschbacher et al.*, 2009].

[43] A marked increase in erosion of the CMC (and basin sedimentation) is evident during a major tectonic event along the SMC in the middle to late Miocene and this is believed to be when formation of the SMC took place. Rapid cooling ages are concentrated on areas governed by strike-slip motion resulting from the transmission of sinistral transpression from the PMFS to the SMC (Tonala shear zone and strike-slip fault of the Tuxtla Malpaso and High Sierra fault systems). This period coincides with major topographic growth and the Chiapas fold-and-thrust belt.

[44] During the Pliocene eastward migration of strike-slip motion took place, from the Tonala shear zone to the strike-slip faults controlling deformation at the Chiapas fold-and-thrust belt and especially to the Tuxtla-Malpaso fault system. Relationships between vertical and horizontal displacement and 6–5 Ma exhumation suggest that the Tuxtla-Malpaso fault system accommodates most of the current motion between the North American and Caribbean plates.

[45] **Acknowledgments.** This work started during a post-doctoral fellowship (C.W.) in the Chaire de Geodynamique of the College de France. We thank the Group of the Americas of TOTAL for founding this work. J. Martinez, L. Andreani and C. Topee are kindly thanked for help in the

field. We want to acknowledge B. Weber, L. Solari, T. Simon-Labric, and Associate Editor L. Rastchbacher for their helpful and constructive reviews; their comments have greatly improved our work.

References

Alzaga-Ruiz, H., M. Lopez, F. Roure, and M. Serane (2009), Interactions between the Laramide foreland and the passive margin of the Gulf of Mexico: Tectonics and sedimentation in the Golden Lane area, Veracruz State, Mexico, *Mar. Pet. Geol.*, *26*, 951–973, doi:10.1016/j.marpetgeo.2008.03.009.

Ambrose, W. A., et al. (2003), Geologic framework of upper Miocene and Pliocene gas splays of the Macuspana basin, southeastern Mexico, *AAPG Bull.*, *87*, 1411–1435, doi:10.1306/04140302022.

Andreani, L., C. Rangin, J. Martínez-Reyes, C. Le Roy, M. Aranda-García, X. Le Pichon, and R. Peterson-Rodriguez (2008a), Neogene left-lateral shearing along the Veracruz Fault: The eastern boundary of the Southern Mexico Block, *Bull. Soc. Geol. Fr.*, *179*, 195–208, doi:10.2113/gssgfbull.179.2.195.

Andreani, L., X. Le Pichon, C. Rangin, and J. Martínez-Reyes (2008b), The southern Mexico block: Main boundaries and new estimation for its Quaternary motion, *Bull. Soc. Geol. Fr.*, *179*, 209–223, doi:10.2113/gssgfbull.179.2.209.

Authemayou, C., G. Brocard, C. Teyssier, T. Simon-Labric, A. Guttiérrez, L. Chiquín, and S. Morán (2011), The Caribbean–North America–Cocos triple junction and the dynamics of the Polochic-Motagua fault systems: Pull-up and zipper models, *Tectonics*, *30*, TC3010, doi:10.1029/2010TC002814.

Carfantan, J. C. (1986), Du système cordillerain Nordamericain au domaine Caraïbe. Etude géologique du Mexique meridional, PhD thesis, 558 pp., Univ. de Savoie, Chambéry, France.

Carter, A., and F. Bristow (2000), Detrital zircon geochronology: Enhancing the quality of sedimentary source information through improved methodology and combined U–Pb and fission-track techniques, *Basin Res.*, *12*, 47–57, doi:10.1046/j.1365-2117.2000.00112.x.

Chavez-Valois, V. M., M. L. C. Valdes, J. I. Juarez Placencia, I. A. Ortiz, M. M. Jurado, R. V. Yanez, M. G. Tristan, and S. Ghosh (2009), A new multidisciplinary focus in the study of the tertiary plays in the Sureste Basin, Mexico, in *Petroleum Systems in the Southern Gulf of Mexico*, edited by C. Bartolini and J. R. Roman Ramos, *AAPG Mem.*, *90*, 155–190.

DeMets, C., R. G. Gordon, D. F. Angus, and C. Stein (1990), Current plate motions, *Geophys. J. Int.*, *101*, 425–478, doi:10.1111/j.1365-246X.1990.tb06579.x.

Dengo, G. (1969), Problems of tectonic relations between Central America and the Caribbean, *Trans. Gulf Coast Assoc. Geol. Soc.*, *19*, 311–320.

Ducea, M., G. Gehrels, S. Shoemaker, J. Ruiz, and V. Valencia (2004), Geologic evolution of the Xolapa complex, southern Mexico: Evidence from U-Pb zircon geochronology, *Geol. Soc. Am. Bull.*, *116*, 1016–1025, doi:10.1130/B25467.1.

Estrada-Carmona, J., B. Weber, L. Hecht, and U. Martens (2009), P-T-t trajectory of metamorphic rocks from the Central Massif Complex: The Custepec Unit, Chiapas, Mexico, *Rev. Mex. Cienc. Geol.*, *26*, 243–259.

Franco, A., E. Molina, H. Lyon-Caen, J. Vergne, T. Monfret, A. Nercessian, S. Cortez, O. Flores, D. Monterosso, and J. Requenna (2009), Seismicity and crustal structure of the Polochic-Motagua fault system area (Guatemala), *Seismol. Res. Lett.*, *80*, 977–984, doi:10.1785/gssrl.80.6.977.

García-Palomo, A., J. L. Macías, and J. M. Espíndola (2004), Strike-slip faults and K-alkaline volcanism at El Chichon volcano, southeastern Mexico, *J. Volcanol. Geotherm. Res.*, *136*, 247–268, doi:10.1016/j.jvolgeores.2004.04.001.

Godínez-Urban, A., T. F. Lawton, R. S. Molina Garza, A. Iriondo, B. Weber, and M. López-Martínez (2011), Jurassic volcanic and sedimentary rocks of the La Silla and Todos Santos Formations, Chiapas: Record of Nazca arc magmatism and rift-basin formation prior to opening of the Gulf of Mexico, *Geosphere*, *7*, 121–144, doi:10.1130/GES00599.1.

Gonzáles-Lara, J. C. (2001), *Le Paleocene du Chiapas (SE du Mexique): Biostratigraphie, Sedimentologie et Stratigraphie Sequentielle*, *Geol. Alp. Mem. HS*, vol. 36, 139 pp., Univ. Joseph Fourier, Grenoble, France.

Guzmán-Speziale, M., and J. J. Meneses-Rocha (2000), The North America–Caribbean plate boundary west of the Motagua-Polochic fault system: A fault jog in southeastern Mexico, *J. South Am. Earth Sci.*, *13*, 459–468, doi:10.1016/S0895-9811(00)00036-5.

Guzmán-Speziale, M., W. Pennington, and T. Matumoto (1989), The triple junction of the North America, Cocos, and Caribbean plates: Seismicity and tectonics, *Tectonics*, *8*, 981–997, doi:10.1029/TC008i005p00981.

Jennette, D., T. Wawrzyniec, K. Fouad, D. Dunlap, X. Meneses-Rocha, F. Grimaldo, R. Munos, D. Barrera, C. Williams-Rojas, and A. Escamilla-Herrera (2003), Traps and turbidite reservoir characteristics from a complex and evolving tectonic setting, Veracruz Basin, southeastern Mexico, *AAPG Bull.*, *87*, 1599–1622, doi:10.1306/05130302010.

Keppie, J. D., and D. J. Moran-Zenteno (2005), Tectonic implications of alternative Cenozoic reconstructions for southern Mexico and the Chortis Block, *Int. Geol. Rev.*, *47*, 473–491, doi:10.2747/0020-6814.47.5.473.

Keppie, J. D., J. Dostal, K. L. Cameron, L. A. Solari, F. Ortega-Gutiérrez, and R. Lopez (2003), Geochronology and geochemistry of Grenvillian igneous suites in the northern Oaxaca Complex, southern Mexico: Tectonic implications, *Precambrian Res.*, *120*, 365–389, doi:10.1016/S0301-9268(02)00166-3.

Ketcham R. (2005), Forward and inverse modeling of low temperature thermochronometry data, in *Thermochronology*, edited by P. W. Reiners and T. A. Ehlers, *Rev. Mineral. Geochem.*, *58*, 275–314.

Ketcham, R. A., A. Carter, R. Donelick, J. Barbarand, and A. Hurford (2007), Improved modeling of fission-track annealing in apatite, *Am. Mineral.*, *92*, 799–810, doi:10.2138/am.2007.2281.

Le Roy, C., C. Rangin, X. Le Pichon, H. Thi Ngoc, L. Andreani, and M. Aranda-Garcia (2008), Neogene crustal shear zone along the western Gulf of Mexico margin and its implications for gravity sliding processes: Evidences from 2D and 3D multichannel seismic data, *Bull. Soc. Geol. Fr.*, *179*, 175–193, doi:10.2113/gssgfbull.179.2.175.

Leroy, S., A. Mauffret, P. Patriat, and M. de Lepinay (2000), An alternative interpretation of the Cayman Trough evolution from a reidentification of magnetic anomalies, *Geophys. J. Int.*, *141*, 539–557, doi:10.1046/j.1365-246x.2000.00059.x.

Lyon-Caen, H., et al. (2006), Kinematics of the North American–Caribbean–Cocos plates in Central America from new GPS measurements across the Polochic-Motagua fault system, *Geophys. Res. Lett.*, *33*, L19309, doi:10.1029/2006GL027694.

Mandujano-Velazquez, J., and D. Keppie (2009), Middle Miocene Chiapas fold and thrust belt of Mexico: A result of collision of the Tehuantepec Transform/Ridge with the Middle America Trench, *Mem. Geol. Soc.*, *327*, 55–69, doi:10.1144/SP327.4.

Mann, P., M. Rogers, and L. Gahagan (2007), Overview of plate tectonic history and its unresolved tectonic problems, in *Geologic and Tectonic Development of the Caribbean Plate Boundary in Northern Central America*, edited by P. Mann, *Spec. Pap. Geol. Soc. Am.*, *428*, 205–241.

Martens, U., B. Weber, and V. Valencia (2010), U-Pb geochronology of Devonian and older Paleozoic beds in the southeastern Maya block, Central America: Its affinity with Peri-Gondwanan terranes, *Geol. Soc. Am. Bull.*, *122*, 815–829, doi:10.1130/B26405.1.

McIntosh, K., E. Silver, and T. Shipley (1993), Evidence and mechanisms for forearc extension at the accretionary Costa Rica convergent margin, *Tectonics*, *12*, 1380–1392, doi:10.1029/93TC01792.

Meneses-Rocha, J. J. (2001), Tectonic evolution of the Ixtapa Graben, an example of a strike-slip basin of southeastern Mexico: Implications for regional petroleum systems, in *The Western Gulf of Mexico Basin: Tectonics, Sedimentary Basins and Petroleum Systems*, edited by C. Bartolini, R. T. Buffler, and A. Cantú-Chapa, *AAPG Mem.*, *75*, 183–216.

Mitra, S., G. Correa-Figueroa, J. Hernandez-Garcia, and A. Murillo-Alvarado (2005), Three-dimensional structural model of the Cantarell and Sihil structures, Campeche bay, Mexico, *AAPG Bull.*, *89*, 1–26, doi:10.1306/08310403108.

Molina-Garza, R., R. Van der Voo, and J. Urrutia-Fucugauchi (1992), Paleomagnetism of the Chiapas Massif, southern Mexico: Evidence for rotation of the Maya block and implications for the opening of the Gulf of Mexico, *Geol. Soc. Am. Bull.*, *104*, 1156–1168, doi:10.1130/0016-7606(1992)104<1156:POTCMS>2.3.CO;2.

Mora, J. C., M. Jaimes-Viera, H. Garduno-Monroy, P. Layer, V. Pompa-Mera, and M. Godinez (2007), Geology and geochemistry characteristics of the Chiapanecan volcanic arc (central area), Chiapas Mexico, *J. Volcanol. Geotherm. Res.*, *162*, 43–72, doi:10.1016/j.jvolgeores.2006.12.009.

Moran-Zenteno, D., D. Keppie, B. Martiny, and E. Gonzáles-Torres (2009), Reassessment of the Paleogene position of the Chortis block relative to southern Mexico: Hierarchical ranking of data and features, *Rev. Mex. Cienc. Geol.*, *26*, 177–188.

Nieto-Samaniego, A. F., S. A. Alaniz-Álvarez, G. Silva-Romo, M. H. Eguiza-Castro, and C. C. Mendoza-Rosales (2006), Latest Cretaceous to Miocene deformation events in the eastern Sierra Madre del Sur, Mexico, inferred from the geometry and age of major structures, *Geol. Soc. Am. Bull.*, *118*, 238–252, doi:10.1130/B25730.1.

Ortega-Gutiérrez, F., L. M. Mitre-Salazar, J. Roldan-Quintana, J. J. Aranda-Gómez, D. Morán-Zenteno, S. A. Alaniz-Alvarez, and A. Nieto-Samaniego (1992), Carta geológica de la República Mexicana, scale 1:2,000,000, Univ. Nac. Auton. de Méx., Inst. de Geol., México City.

Ortega-Gutiérrez, F., J. Ruiz, and E. Centeno-Garcia (1995), Oaxaquia, a Proterozoic microcontinent accreted to North America during the late Paleozoic, *Geology*, *23*, 1127–1130, doi:10.1130/0091-7613(1995)023<1127:OAPMAT>2.3.CO;2.

Ortega-Gutiérrez, F., L. Solari, C. Ortega-Obregón, M. Elías-Herrera, U. Martens, S. Moral-Icál, M. Chiquín, J. Duncan Keppie, R. Torres de León,

and P. Schaaf (2007), The Maya-Chortis boundary: A tectonostratigraphic approach, *Int. Geol. Rev.*, *49*, 996–1024, doi:10.2747/0020-6814.49.11.996.

Pérez-Gutiérrez, R., L. A. Solari, A. Gómez-Tuena, and V. A. Valencia (2009), El terreno Cuicateco: ¿cuenca oceánica con infl uencia de subducción del Cretácico Superior en el sur de México? Nuevos datos estructurales, geoquímicos y geocronológicos, *Rev. Mex. Cienc. Geol.*, *26*, 222–242.

Pindell, J. L., and L. Kennan (2009), Tectonic evolution of the Gulf of Mexico, Caribbean and northern South America in the mantle reference frame: An update, in *The Origin and Evolution of the Caribbean Plate*, edited by K. James, M. Lorente, and J. Pindell, *Geol. Soc. Spec. Publ.*, *328*, 1–55, doi:10.1144/SP328.1.

Pindell, J., L. Kennan, and S. Barrett (2000), Putting it all together again, *AAPG Explor.*, *21*, 34–37.

Pindell, J., L. Kennan, K. P. Stanek, W. V. Maresch, and G. Draper (2006), Foundations of Gulf of Mexico and Caribbean evolution: Eight controversies resolved, *Geol. Acta*, *4*, 303–341.

Quezada-Muñeton (1987), El Cretacico Medio-Superior y el limite Cretacico Superior-Terciario inferior en la Sierra de Chiapas, *Bol. Assoc. Mex. Geol. Petrol.*, *39*, 3–98.

Rangin, C., X. Le Pichon, J. Martinez-Reyes, and M. Aranda-Garcia (2008), Gravity tectonics and plate motion: The western margin of the Gulf of Mexico: Introduction, *Bull. Soc. Geol. Fr.*, *179*, 107–116, doi:10.2113/gssgfbull.179.2.107.

Ratschbacher, L., et al. (2009), The North American-Caribbean plate boundary in Mexico-Guatemala-Honduras, in *The Origin and Evolution of the Caribbean Plate*, edited by K. James, M. Lorente, and J. Pindell, *Geol. Soc. Spec. Publ.*, *328*, 219–293. doi:10.1144/SP328.11.

Rogers, R. D., P. Mann, and P. Emme (2007), Tectonic terranes of the Chortis block based on integration of regional aeromagnetic and geologic data, in *Geologic and Tectonic Development of the Caribbean Plate Boundary in Northern Central America*, edited by P. Mann, *Spec. Pap. Geol. Soc. Am.*, *428*, 65–88.

Rosencrantz, E., and J. G. Sclater (1986), Depth and age in the Cayman Trough, *Earth Planet. Sci. Lett.*, *79*, 133–144, doi:10.1016/0012-821X(86)90046-4.

Sanchez Montes de Oca, R. (2006), Curso Cuenca del Sureste, report, 296 pp., Petrol. Mex., Mexico City.

Solari, L. A., J. D. Keppie, F. Ortega-Gutiérrez, K. Cameron, and R. Lopez (2004), ~990 Ma peak granulitic metamorphism and amalgamation of Oaxaquia, Mexico: U-Pb zircon geochronological and common Pb isotopic data, *Rev. Mex. Cienc. Geol.*, *21*, 212–225.

Solari, L. A., R. Torres de León, G. Hernández Pineda, J. Solé, G. Solís-Pichardo, and G. Hernánde-Treviño (2007), Tectonic significance of Cretaceous–Tertiary magmatic and structural evolution of the northern margin of the Xolapa Complex, Tierra Colorada area, southern Mexico, *Geol. Soc. Am. Bull.*, *119*, 1265–1279, doi:10.1130/B26023.1.

Solari, L. A., F. Ortega-Gutiérrez, M. Elias-Herrera, P. Schaaf, M. Norman, R. Torres de Leon, C. Ortega-Obregon, M. Chiquin and S. Morán-Icál (2009), U-Pb zircon geochronology of Palaeozoic units in western and central Guatemala: Insights into the tectonic evolution of Middle America, *Geol. Soc. Spec. Publ.*, *328*, 295–313, doi:10.1144/SP328.12.

Storti, F., R. E. Holdsworth, and F. Salvini (2003), Intraplate strike-slip deformation belts, *Geol. Soc. Spec. Publ.*, *210*, 1–14, doi:10.1144/GSL.SP.2003.210.01.01.

Torres de León, R., L. Solari, F. Ortega-Gutiérrez, and U. Martens (2012), The Chortis block–southwestern Mexico connections: U-Pb zircón geochronology constraints, *Am. J. Sci.*, *312*, 288–313, doi:10.2475/03.2012.02.

Vermeesch, P. (2004), How many grains are needed for a provenance study?, *Earth Planet. Sci. Lett.*, *224*, 441–451, doi:10.1016/j.epsl.2004.05.037.

Vermeesch, P. (2012), On the visualisation of detrital age distributions, *Chem. Geol.*, *312–313*, 190–194, doi:10.1016/j.chemgeo.2012.04.021.

Wawrzyniec, T. (2005), A newly discovered, relic, transcurrent plate boundary—The Tonala shear zone and paleomagnetic evaluation of the western Maya block, SW Mexico, Paper 28–52005 presented at Salt Lake City Annual Meeting, Geol. Soc. of Am., Salt Lake City, Utah.

Weber, B., and L. Hecht (2003), Petrology and geochemistry of metaigneous rocks from a Grenvillian basement fragment in the Maya block: The Guichicovi complex, Oaxaca, southern Mexico, *Precambrian Res.*, *124*, 41–67.

Weber, B., and H. Kohler (2009), Sm–Nd, Rb–Sr and U–Pb geochronology of a Grenville Terrane in Southern Mexico: origin and geologic history of the Guichicovi Complex, *Prec. Res.*, *96*, 245–262.

Weber, B., A. Iriondo, W. Premo, L. Hecht, and P. Schaaf (2007), New insights into the history and origin of the southern Maya block, SE Mexico: U-Pb-SHRIMP zircon geochronology from metamorphic rocks of the Chiapas massif, *Int. J. Earth Sci.*, *96*, 253–269, doi:10.1007/s00531-006-0093-7.

Weber, B., V. A. Valencia, P. Schaaf, V. Pompa-Mera, and J. Ruiz (2008), Significance of provenance ages from the Chiapas massif complex (SE Mexico): Redefining the Paleozoic basement of the Maya block and its evolution in a peri-Gondwanan entourage, *J. Geol.*, *116*, 619–639, doi:10.1086/591994.

Wilson, D. (1996), Fastest known spreading on the Miocene Cocos-Pacific plate boundary, *Geophys. Res. Lett.*, *23*, 3003–3006, doi:10.1029/96GL02893.

Witt, C., C. Rangin, L. Andreani, N. Olaez, and J. Martinez (2012), The transpressive left-lateral Sierra Madre de Chiapas and its buried front in the Tabasco Plain (south Mexico), *J. Geol. Soc.*, *169*, 143–155, doi:10.1144/0016-76492011-024.